The Berry Phase in Magnetism and the Anomalous Hall Effect

Patrick Bruno

Max-Planck-Institut für Mikrostrukturphysik, Halle, Germany

1 INTRODUCTION

In 1983, Berry made the surprising discovery that a quantum system adiabatically transported round a closed circuit C in the space of external parameters acquires, besides the familiar dynamical phase, a nonintegrable phase depending only on the geometry of the circuit C (Berry, 1984). This Berry phase, which had been overlooked for more than half a century, provides us a very deep insight into the geometric structure of quantum mechanics and gives rise to various observable effects. The concept of the Berry phase has now become a central unifying concept in quantum mechanics, with applications in fields ranging from chemistry to condensed-matter physics (Shapere and Wilczek, 1989; Bohm *et al.*, 2003).

The aim of this article is to give an elementary introduction to the Berry phase, and to discuss its various implications in the field of magnetism, where it plays an increasingly important role. The reader is referred to specialized textbooks (Shapere and Wilczek, 1989; Bohm *et al.*, 2003) for a more comprehensive presentation of the field of geometrical phases. Particular emphasis will be given to the discussion of the anomalous Hall effect, the theory of which has been considerably renewed recently, on the basis of the concept of Berry phase.

2 PARALLEL TRANSPORT IN GEOMETRY

The importance of the Berry phase stems from the fact that it reveals the intimate geometrical structure underlying quantum mechanics. It is therefore appropriate to start with an introduction to the fundamental concept of *parallel transport* in a purely geometrical context; here, we follow the discussion given by Berry (1990).

This is best illustrated by means of a simple example. Consider a surface Σ (e.g., a plane, a sphere, a cone, etc.) and a vector constrained to lie everywhere in the plane tangent to the surface. Next, we wish to transport the vector on the surface, *without rotating it around the axis normal to the surface*, as illustrated in Figure 1. We are interested, in particular, in the case, in which the arrow is transported round a closed circuit $C \equiv (1 \rightarrow 2 \rightarrow 3 \rightarrow 1)$. We may encounter two different situations: (i) if the surface is flat,

Handbook of Magnetism and Advanced Magnetic Materials. Edited by Helmut Kronmüller and Stuart Parkin. Volume 1: *Fundamentals and Theory*. ISBN: 978-0-470-02217-7.

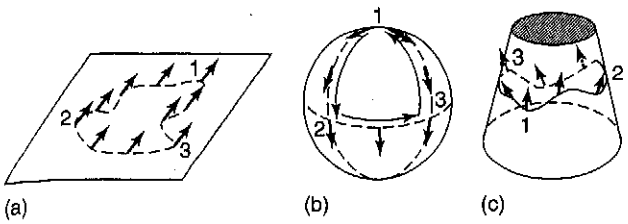

Figure 1. Sketch of parallel transport on (a) a plane, (b) a sphere, and (c) a cone.

as in Figure 1(a), then the arrow always remains parallel to its original orientation, and is, therefore, unchanged after completion of the circuit C; (ii) if, however, the surface Σ is curved as in Figure 1(b) and (c), the arrow, being constrained to lie in the local tangent plane, cannot remain parallel to its original orientation, and after completion of the circuit C, has clearly undergone a rotation by an angle $\theta(C)$, a phenomenon referred to as *anholonomy*.

Let us now formalize this procedure. The arrow is represented by a tangent unit vector $\mathbf{e}^1$, transported along a circuit $C \equiv \{\mathbf{r}(t)|t = 0 \to T\}$ on the surface. Defining $\mathbf{n}(\mathbf{r})$ as the unit vector normal to the surface at point $\mathbf{r}$, we define a second tangent unit vector $\mathbf{e}^2 \equiv \mathbf{n} \times \mathbf{e}^1$, which is also parallel transported on the surface along C. The three unit vectors $(\mathbf{n}, \mathbf{e}^1, \mathbf{e}^2)$ form an orthonormal reference frame. As $\mathbf{e}^1$ and $\mathbf{e}^2$ are transported, they have to rotate with an angular velocity $\boldsymbol{\omega}$ (to be determined) if the surface is not flat, that is, the equation of motion of $\mathbf{e}^1$ and $\mathbf{e}^2$ is

$$\dot{\mathbf{e}}^r = \boldsymbol{\omega} \times \mathbf{e}^r \quad (r = 1, 2) \tag{1}$$

where the overdot indicates the time derivative. One can easily see that in order to fulfill the requirements that $\mathbf{e}^1$ and $\mathbf{e}^2$ remain tangent unit vectors (i.e., $\mathbf{e}^r \cdot \mathbf{n} = 0$, $(r = 1, 2)$) and never rotate around $\mathbf{n}$ (i.e., $\boldsymbol{\omega} \cdot \mathbf{n} = 0$), the angular velocity has to be given by

$$\boldsymbol{\omega} = \mathbf{n} \times \dot{\mathbf{n}} \tag{2}$$

The law of parallel transport is therefore,

$$\dot{\mathbf{e}}^r = (\mathbf{n} \times \dot{\mathbf{n}}) \times \mathbf{e}^r = -(\mathbf{e}^r \cdot \dot{\mathbf{n}})\mathbf{n} \tag{3}$$

This law can be expressed in a form more suitable for generalization to the case of quantum mechanics, by defining the complex unit vector,

$$\boldsymbol{\phi} \equiv \frac{\mathbf{e}^1 + \mathrm{i}\mathbf{e}^2}{\sqrt{2}} \tag{4}$$

with

$$\boldsymbol{\phi}^\star \cdot \boldsymbol{\phi} = 1 \tag{5}$$

The law of parallel transport now reads,

$$\boldsymbol{\phi}^\star \cdot \dot{\boldsymbol{\phi}} = 0 \tag{6}$$

In order to express the rotation of the unit vectors $(\mathbf{e}^1, \mathbf{e}^2)$ as they move around C, we need to choose a *fixed* local orthonormal frame $(\mathbf{n}(\mathbf{r}), \mathbf{t}^1(\mathbf{r}), \mathbf{t}^2(\mathbf{r}))$ on the surface. The normal unit vector $\mathbf{n}(\mathbf{r})$ is, of course, uniquely determined by the surface, but we have an infinity of possible choices for $\mathbf{t}^1(\mathbf{r})$ (we simply impose that it is a smooth function of $\mathbf{r}$), which corresponds to a gauge freedom; once we have made a choice for $\mathbf{t}^1(\mathbf{r})$, then $\mathbf{t}^2(\mathbf{r})$ is of course uniquely determined. We next define the complex unit vector,

$$\mathbf{u}(\mathbf{r}) \equiv \frac{\mathbf{t}^1(\mathbf{r}) + \mathrm{i}\mathbf{t}^2(\mathbf{r})}{\sqrt{2}} \tag{7}$$

with, of course,

$$\mathbf{u}^\star(\mathbf{r}) \cdot \mathbf{u}(\mathbf{r}) = 1 \tag{8}$$

The relation between the parallel transported frame and the fixed one is expressed as

$$\boldsymbol{\phi}(t) = \exp[-\mathrm{i}\theta(t)]\ \mathbf{u}(\mathbf{r}(t)) \tag{9}$$

where $\theta(t)$ is the angle by which $(\mathbf{t}^1, \mathbf{t}^2)$ must be rotated to coincide with $(\mathbf{e}^1, \mathbf{e}^2)$. We obtain the equation satisfied by $\theta(t)$ by inserting the preceding definition in the equation of parallel transport (6), and obtain

$$0 = \boldsymbol{\phi}^\star \cdot \dot{\boldsymbol{\phi}} = -\mathrm{i}\dot{\theta}\mathbf{u}^\star \cdot \mathbf{u} + \mathbf{u}^\star \cdot \dot{\mathbf{u}} \tag{10}$$

Since $\mathbf{u}^\star \cdot \mathbf{u} = 1$ and $\mathbf{u}^\star \cdot \dot{\mathbf{u}}$ is imaginary, we get

$$\dot{\theta} = \mathrm{Im}(\mathbf{u}^\star \cdot \dot{\mathbf{u}}) \tag{11}$$

so that

$$\theta(C) = \mathrm{Im} \oint_C \mathbf{u}^\star \cdot \mathrm{d}\mathbf{u} \tag{12}$$

$$= -\oint_C \mathbf{t}^2 \cdot \mathrm{d}\mathbf{t}^1 \tag{13}$$

If we choose a coordinate system (X_1, X_2) on our surface Σ and define the vector field $\mathbf{A}(\mathbf{r})$ (usually called a *connection*) on Σ as

$$A_i(\mathbf{X}) \equiv \mathrm{Im}\left[u_j^\star(\mathbf{X}) \frac{\partial u_j(\mathbf{X})}{\partial X_i}\right] \tag{14}$$

where we have used Einstein's convention of summation over repeated indices, we get

$$\theta(C) = \oint_C \mathbf{A}(\mathbf{X}) \cdot \mathrm{d}\mathbf{X} \tag{15}$$

which constitutes the *1-form* expression of the anholonomy angle $\theta(C)$. The connection $\mathbf{A}(\mathbf{X})$ depends on our particular gauge choice for $\mathbf{t}^1(\mathbf{X})$: if we make a new choice $\mathbf{t}^{1'}(\mathbf{X})$ which is brought in coincidence with $\mathbf{t}^1(\mathbf{X})$ by a rotation of angle $\mu(\mathbf{X})$, that is, if we make the gauge transformation

$$\mathbf{u}(\mathbf{X}) \to \mathbf{u}'(\mathbf{X}) \equiv \exp(-\mathrm{i}\mu(\mathbf{X}))\,\mathbf{u}(\mathbf{X}) \tag{16}$$

we obtain a new connection

$$A'_i(\mathbf{X}) \equiv \mathrm{Im}\left[u^*_{j'}(\mathbf{X})\frac{\partial u_{j'}(\mathbf{X})}{\partial X_i}\right] = A_i(\mathbf{X}) - \frac{\partial \mu(\mathbf{X})}{\partial X_i} \tag{17}$$

However, since

$$\oint_C \nabla\mu(\mathbf{r}) \cdot \mathrm{d}\mathbf{r} = \oint_C \mathrm{d}\mu(\mathbf{r}) = 0 \tag{18}$$

we can see that the expression (15) for the anholonomy angle $\theta(C)$ is indeed gauge invariant, as it should be.

A more intuitive understanding of the anholonomy angle may be obtained if we use Stokes' theorem to express it as a surface integral. In doing so, however, we should pay attention to the possible existence of holes in the surface Σ. If this is the case, Σ is said to be nonsimply connected. An example is sketched in Figure 2, where the surface Σ has two holes limited by the contours C_1 and C_2 (hatched areas in Figure 2). Applying Stokes' theorem, we then obtain

$$\theta(C) = \iint_S B(\mathbf{X})\mathrm{d}X_1\,\mathrm{d}X_2 + \sum_i N_i(C)\theta(C_i) \tag{19}$$

where the surface S is the subset of the surface Σ that is limited by the circuit (dotted area in Figure 2), C, $N_i(C)$ is the winding number of circuit C around the hole i (i.e., the difference between the number of turns in counterclockwise and clockwise directions),

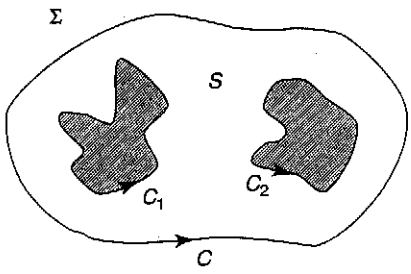

Figure 2. Sketch of a nonsimply connected surface Σ, with two holes (hatched areas), limited by the contours C_1 and C_2.

$$\theta(C_i) \equiv \oint_{C_i} \mathbf{A}(\mathbf{X}) \cdot \mathrm{d}\mathbf{X} \tag{20}$$

is the anholonomy angle of circuit C_i and

$$B(\mathbf{X}) \equiv \left(\frac{\partial A_2}{\partial X_1} - \frac{\partial A_1}{\partial X_2}\right) = \mathrm{Im}\left[\frac{\partial \mathbf{u}^*}{\partial X_1} \cdot \frac{\partial \mathbf{u}}{\partial X_2} - \frac{\partial \mathbf{u}^*}{\partial X_2} \cdot \frac{\partial \mathbf{u}}{\partial X_1}\right] \tag{21}$$

Equation (19) constitutes the *2-form* expression of the anholonomy angle $\theta(C)$. One can see immediately that, unlike the connection $\mathbf{A}(\mathbf{X})$, the quantity $B(\mathbf{X})$ is gauge invariant. The geometrical meaning of $B(\mathbf{X})$ stems from its relation to the *Gaussian curvature* K of Σ at point $\mathbf{X}$, that is,

$$B(\mathbf{X})\mathrm{d}X_1\mathrm{d}X_2 = K\mathrm{d}S \equiv \frac{\mathrm{d}S}{R_1(\mathbf{X})\,R_2(\mathbf{X})} \tag{22}$$

where $R_1(\mathbf{X})$ and $R_2(\mathbf{X})$ are the principal curvature radii at point $\mathbf{X}$. In the case of the sphere, this is easily checked by explicit calculation, taking the usual spherical angles (θ, φ) as variables (X_1, X_2). Since the Gaussian curvature is related to the solid angle Ω spanned by the normal unit vector $\mathbf{n}$ by

$$B = \frac{\mathrm{d}^2\Omega}{\mathrm{d}X_1\,\mathrm{d}X_2} \tag{23}$$

we finally get

$$\theta(C) - \sum_i N_i(C)\theta(C_i) = \iint_S \frac{\mathrm{d}^2\Omega}{\mathrm{d}X_1\,\mathrm{d}X_2}\mathrm{d}X_1\,\mathrm{d}X_2 = \iint_S \mathrm{d}^2\Omega = \Omega(S) \tag{24}$$

where $\Omega(S)$ is the solid angle described by the normal vector $\mathbf{n}$ on the surface S. That the above results hold not only for a sphere but also for any surface can be understood easily from the following argument: Equation (3) shows that the trajectory of the parallel transported tangent vectors is entirely determined by the trajectory of the normal unit vector $\mathbf{n}$ along C. We can therefore map the trajectory C on the surface Σ to a trajectory C' on the sphere of unit radius S^2, by mapping each point of Σ onto the point of S^2 with the same normal vector $\mathbf{n}$. This implies that we can restrict ourselves to studying the case of parallel transport on S^2 and obtain conclusions valid for parallel transport on any surface Σ.

Let us examine these results for the examples sketched in Figure 1. For the case of the plane, the anholonomy of course trivially vanishes. For the sphere, the anholonomy angle is

given by the solid angle $\Omega(S)$ and is therefore a *geometric* property of the circuit C; this can easily be checked through the following experiment: take your pen in you left hand, and raise your arm above you head, the pen pointing in front of you; then rotate your arm until it is horizontal in front of you, without twisting your hand; then rotate it by 90° to your left; finally rotate your arm back to the vertical (pay attention to never twist your hand in whole process); the pen is now pointing to your left, that is, it has rotated by $4\pi/8 = \pi/2$. For the case of the cone, the Gaussian curvature vanishes everywhere (a cone can be fabricated by rolling a sheet of paper), so that the anholonomy angle is in fact a *topological* property of the circuit C, given by the winding number of the circuit C around the cone (multiplied by the solid angle of the cone).

3 PARALLEL TRANSPORT IN CLASSICAL MECHANICS: FOUCAULT'S PENDULUM AND THE GYROSCOPE

Let us now consider the famous experiment of Foucault's pendulum that demonstrated the earth's rotation. If the pendulum trajectory is originally planar (swinging oscillation), the vertical component of the angular momentum vanishes. Since forces exerted on the pendulum (gravity and wire tension) produce a vanishing vertical torque, the vertical component of the angular momentum has to be conserved. The absence of any vertical torque imposes that the swing plane has to follow a law of parallel transport as the direction of gravity slowly changes because of the earth's rotation. Therefore, within 1 day it rotates by an angle equal to the solid angle described by the vertical $2\pi(1 - \cos\theta)$, where θ is the colatitude.

The parallel transport may also affect the phase of the periodic motion of the Foucault pendulum or the rotation phase of a gyroscope. Let us consider a gyroscope whose rotation axis is constrained to remain parallel to the axis $\mathbf{n}$; let us now move the rotation axis $\mathbf{n}$ round a closed circuit C. The rotation angle of the gyroscope will be the sum of the *dynamic rotation angle* ωt and the *geometric anholonomy angle* $\theta(C)$ equal to the solid angle described by the rotation axis. Thus if we have two synchronous gyroscopes and perform different circuits with the rotation axes, they will eventually be dephased with respect to each other, an effect that could easily be observed by stroboscopy. This geometric anholonomy angle is known as *Hannay's angle* (Hannay, 1985; Berry, 1985). If the Foucault pendulum is given a conical oscillation instead of a planar swing, then we have exactly the same situation as described in the preceding text for the gyroscope, and the rotation angle will have an anholonomy excess angle given by the solid angle described by the vertical. Thus, two identical Foucault pendula (i.e., of same length) with circular oscillations in opposite directions will have slightly different oscillation frequencies and will progressively get dephased with respect to each other. The swinging motion of the usual Foucault may be viewed as the superposition of circular motions in opposite directions, so that the rotation of the swinging plane may be viewed as resulting from the previously mentioned frequency shift.

4 PARALLEL TRANSPORT IN QUANTUM MECHANICS: THE BERRY PHASE

Let us now consider a quantum mechanical system described by a Hamiltonian controlled by a set of external parameters $(R_1, R_2, \ldots)$, which we describe collectively as a vector $\mathbf{R}$ in some abstract parameter space. Physically, the external parameters may be magnetic or electric fields, and so on. For each value $\mathbf{R}$ of the external parameters, the Hamiltonian $H(\mathbf{R})$ has eigenvalues $E_n(\mathbf{R})$ and eigenvectors $|n(\mathbf{R})\rangle$ satisfying the independent Schrödinger equation, that is,

$$H(\mathbf{R})\,|n(\mathbf{R})\rangle = E_n(\mathbf{R})\,|n(\mathbf{R})\rangle \tag{25}$$

The eigenvectors $|n(\mathbf{R})\rangle$ are defined up to an arbitrary phase, and there is *a priori* no particular phase relation between eigenstates corresponding to different values of the parameter $\mathbf{R}$. We make a particular choice for the phase of the eigenstates, simply requiring that $|n(\mathbf{R})\rangle$ varies smoothly with $\mathbf{R}$ in the region of interest. It may happen that the eigenstates we have chosen are not single-valued functions of $\mathbf{R}$. If this happens, special care must be given to this point.

Let us perform an adiabatic closed circuit $\mathcal{C} \equiv \{\mathbf{R}(t) | t = 0 \to T\}$ in the parameter space. The adiabatic theorem (Messiah, 1991) tells us that if the rate of variation of the external parameters is low enough, a system that is initially in the nth stationary state $|n\rangle$ (assumed nondegenerate) of the Hamiltonian will remain continuously in the state $|n\rangle$. The condition of adiabaticity is that the stationary state under consideration remains nondegenerate, and the rate of variation of the Hamiltonian is low enough to make the probability of transition to another state $|m\rangle$ vanishingly small, that is,

$$\hbar|\langle m|\dot{H}|n\rangle| \ll |E_m - E_n|^2 \quad \forall m \neq n \tag{26}$$

Then of course, if one performs a closed adiabatic circuit $\mathcal{C}$, the system has to return to its original state.

Berry (1984) asked the following question: what will be the phase of the state after completion of the circuit C? It may be difficult at first sight to realize that this question may be of any interest. Indeed, the expectation value of any observable quantity A,

$$\langle A \rangle \equiv \langle \psi | A | \psi \rangle \tag{27}$$

does not depend on the phase of $|\psi\rangle$. This lack of interest is certainly the main reason why the Berry phase was (almost) completely overlooked for more than half a century of quantum mechanics. One should mention here that there has been, prior to Berry's seminal paper (Berry, 1984), a number of precursor works on effects related to the Berry phase, including, notably, Pancharatnam's work on optical polarization (Pancharatnam, 1956), Aharonov and Bohm's work on the phase due to the electromagnetic potential vector (Aharonov and Bohm, 1959), and Mead and Truhlar's work on the molecular Aharonov–Bohm effect in the Born–Oppenheimer theory of molecular vibrations (Mead and Truhlar, 1979). However, Berry (1984) was the first to point out the geometric significance and the generality of the adiabatic geometric phase. After the publication of Berry's paper, the generality and the fecundity of this new concept has been widely recognized, soon leading to a considerable amount of developments (Shapere and Wilczek, 1989; Bohm *et al.*, 2003).

So, following Berry, taking

$$|\psi(t=0)\rangle \equiv |n(\mathbf{R}(t=0))\rangle \tag{28}$$

we express the state $|\psi(t)\rangle$ at a latter time t as

$$|\psi(t)\rangle \equiv \exp\left[\frac{-\mathrm{i}}{\hbar}\int_0^t \mathrm{d}t'\, E_n(\mathbf{r}(t'))\right]|\phi_n(t)\rangle \tag{29}$$

that is, we introduce an auxiliary wave function $|\phi_n(t)\rangle$ with a zero dynamical phase. Using the time-dependent Schrödinger equation,

$$\mathrm{i}\hbar|\dot{\psi}(t)\rangle = H(t)|\psi(t)\rangle \tag{30}$$

and projecting it on $\langle\psi(t)|$, we get

$$\begin{aligned} 0 &= \langle\psi(t)|\left(H(t) - \mathrm{i}\hbar\frac{\partial}{\partial t}\right)|\psi(t)\rangle \\ &= \langle\phi_n(t)|\dot{\phi}_n(t)\rangle \end{aligned} \tag{31}$$

where we have used the relation

$$\langle\psi(t)|H(t)|\psi(t)\rangle = E_n(t) \tag{32}$$

which follows from the adiabatic theorem. Equation (31) shows that the wave function $|\phi_n(t)\rangle$ obeys a quantum mechanical analog of the law of parallel transport (6).

In complete analogy with the problem of parallel transport on a surface, we now express the parallel transported state $|\phi_n(t)\rangle$ in terms of the fixed eigenstates $|n(\mathbf{R})\rangle$ as

$$|\phi_n(t)\rangle \equiv \exp((\mathrm{i}\gamma_n(t))\,|n(\mathbf{R})\rangle \tag{33}$$

where the phase $\gamma_n(t)$ plays the same role as the angle $-\theta(t)$ for the problem of parallel transport on a surface. We then immediately get the equation of motion of $\gamma_n(t)$, that is,

$$\dot{\gamma}_n(t) = \mathrm{i}\langle n|\dot{n}\rangle = -\mathrm{Im}\langle n(\mathbf{R}(t))|\frac{\mathrm{d}}{\mathrm{d}t}n(\mathbf{R}(t))\rangle \tag{34}$$

which is analogous to equation (11).

Finally, the answer to the question originally asked by Berry is

$$|\psi(T)\rangle = \exp\left[\mathrm{i}(\delta_n + \gamma_n(C))\right]|\psi(0)\rangle \tag{35}$$

where

$$\delta_n \equiv \frac{-1}{\hbar}\int_0^T E_n(\mathbf{R}(t))\,\mathrm{d}t \tag{36}$$

is the dynamical phase, and

$$\gamma_n(C) \equiv -\mathrm{Im}\left[\oint_C \langle n(\mathbf{R})|\partial_{\mathbf{R}}|n(\mathbf{R})\rangle\cdot\mathrm{d}\mathbf{R}\right] - \alpha_n(C) \tag{37}$$

is the Berry phase. The last term in the latter equation arises when the states $|n(\mathbf{R})\rangle$ are not a single-valued function of $\mathbf{R}$ in the region of interest of the parameter space and is given by

$$\alpha_n(C) = \mathrm{i}\ln\left[\langle n(\mathbf{R}(0))|n(\mathbf{R}(T))\rangle\right] \tag{38}$$

Note that this term was absent in Berry's original paper (Berry, 1984), because the basis states $|n(\mathbf{R})\rangle$ were assumed to be single valued. We shall omit this term in the subsequent text, and consider only the case of single-valued basis states.

We note the very close analogy between the results obtained for quantum and classical systems. The dynamical phase of a quantum system is analogous to the rotation angle ωT in classical mechanics, whereas the Berry phase is analogous to Hannay's angle (they both arise from the anholonomy of parallel transport).

Defining the connection $\mathbf{A}^n(\mathbf{R})$ as

$$\mathbf{A}^n(\mathbf{R}) \equiv -\mathrm{Im}\left[\langle n(\mathbf{R})|\partial_{\mathbf{R}}n(\mathbf{R})\rangle\right] \tag{39}$$

we reexpress the Berry phase as

$$\gamma_n(C) \equiv \oint_C \mathbf{A}^n(\mathbf{R}) \cdot \mathrm{d}\mathbf{R} \tag{40}$$

which constitutes the 1-form expression of the Berry phase. The latter clearly depends only on the geometry of the circuit C. The connection $\mathbf{A}^n(\mathbf{R})$ is not gauge invariant – if we make a new choice for the phase of the reference state, that is,

$$|n(\mathbf{R})\rangle' = \exp(-i\mu(\mathbf{R}))|n(\mathbf{R})\rangle \tag{41}$$

with a single-valued function $\mu(\mathbf{R})$, we obtain a different connection

$$\mathbf{A}^{n\prime}(\mathbf{R}) = \mathbf{A}^n(\mathbf{R}) + \partial_{\mathbf{R}}\mu(\mathbf{R}) \tag{42}$$

However, the Berry phase $\gamma_n(C)$ is gauge invariant, as it should be.

As for the geometric parallel transport on surfaces, we may obtain a gauge-invariant and more transparent expression by transforming the preceding result to a surface integral using Stokes' theorem. Here too, we have to pay attention to the existence of holes in the parameter space – if the parameter space is multiply connected, and if the circuit C cannot be continuously deformed to a point (i.e., it is not *homotopic* to a point), we must take into account terms associated with the winding of C around holes of the parameter space.

The formulation of the Berry phase as a surface integral in a form that is independent of a particular choice of coordinates of the parameter space generally requires the use of mathematical formalism of differential forms (Bohm *et al.*, 2003), which is beyond the scope of this article. We can nevertheless obtain a useful result without resorting to any advanced mathematics if we make a suitable choice of coordinates of the parameter space. Let us choose a surface $\mathcal{S}$ in the parameter space which is bound by the circuit C, and a parameterization (R_1, R_2) of the surface $\mathcal{S}$. Using Stokes' theorem, we then get

$$\gamma_n(C) = \iint_{\mathcal{S}} B^n(\mathbf{R})\mathrm{d}R_1\,\mathrm{d}R_2 + \sum_i N_i(C)\gamma_n(C_i) \tag{43}$$

where C_i are the circuits bounding the holes of the parameter space and N_i, the corresponding winding numbers of the circuit C around them, and where

$$\begin{aligned} B^n(\mathbf{R}) &\equiv \left(\partial_{R_1}A_2^n - \partial_{R_2}A_1^n\right) \\ &= -\mathrm{Im}\left[\langle\partial_{R_1} n(\mathbf{R})|\partial_{R_2}n(\mathbf{R})\rangle - \langle\partial_{R_2} n(\mathbf{R})|\partial_{R_1}n(\mathbf{R})\rangle\right] \end{aligned} \tag{44}$$

is the *Berry curvature*. In the case where the parameter space is three-dimensional, we can use the familiar language of vector calculus, as in electrodynamics, and Stokes' theorem yields

$$\gamma_n(C) = \iint_{\mathcal{S}} \mathbf{B}^b(\mathbf{R}) \cdot \mathbf{n}\,\mathrm{d}S + \sum_i N_i(C)\gamma_n(C_i) \tag{45}$$

$$\begin{aligned} \mathbf{B}^n(\mathbf{R}) &\equiv \nabla \times \mathbf{A}^n(\mathbf{R}) \\ &= -\mathrm{Im}\left[\langle\nabla n(\mathbf{R})| \times |\nabla n(\mathbf{R})\rangle\right] && (46) \\ &= -\mathrm{Im}\sum_{m\neq n}\langle\nabla n(\mathbf{R})|m(\mathbf{R})\rangle \times \langle m(\mathbf{R})|\nabla n(\mathbf{R})\rangle && (47) \end{aligned}$$

Making use of the relation

$$\langle m|\nabla n\rangle = \frac{\langle m|\nabla H|n\rangle}{E_n - E_m} \tag{48}$$

one eventually gets

$$\mathbf{B}^n(\mathbf{R}) = -\mathrm{Im}\sum_{m\neq n} \times \frac{\langle n(\mathbf{R})|\nabla H(\mathbf{R})|m(\mathbf{R})\rangle \times \langle m(\mathbf{R})|\nabla H(\mathbf{R})|n(\mathbf{R})\rangle}{(E_m(\mathbf{R}) - E_n(\mathbf{R}))^2} \tag{49}$$

Obviously, the Berry curvature is gauge invariant. As the notation suggests, the Berry curvature $\mathbf{B}^n$ plays the role of a magnetic field in the space of parameters, whose vector potential is the Berry connection $\mathbf{A}^n$.

The energy denominator in equation (49) shows that if the circuit C lies in a region of the parameter space that is close to a point $\mathbf{R}^\star$ of twofold degeneracy involving the two states labeled + and −, the corresponding Berry connections $\mathbf{B}_+$ and $\mathbf{B}_-$ are dominated by the term involving the denominator $(E_+ - E_-)^2$ and the contribution involving other states can be neglected. So, to first order in $\mathbf{R} - \mathbf{R}^\star$, one has

$$\mathbf{B}_+(\mathbf{R}) = -\mathbf{B}_-(\mathbf{R}) = -\mathrm{Im} \times \frac{\langle +(\mathbf{R})|\nabla H(\mathbf{R}^\star)| -(\mathbf{R})\rangle \times \langle -(\mathbf{R})|\nabla H(\mathbf{R}^\star)| +(\mathbf{R})\rangle}{(E_+(\mathbf{R}) - E_-(\mathbf{R}))^2} \tag{50}$$

The general form of the Hamiltonian $H(\mathbf{R})$ of a two-level system is (without loss of generality, we may take $\mathbf{R}^\star = 0$)

$$H(\mathbf{R}) \equiv \frac{1}{2}\begin{pmatrix} Z & X - \mathrm{i}Y \\ X + \mathrm{i}Y & -Z \end{pmatrix} \tag{51}$$

with eigenvalues

$$E_+(\mathbf{R}) = -E_-(\mathbf{R}) = \frac{1}{2}R \tag{52}$$

This illustrates a theorem due to von Neumann and Wigner (1929), stating that it is necessary to adjust three independent parameters in order to obtain a twofold degeneracy from a Hermitian matrix. The gradient of the Hamiltonian is

$$\nabla H = \frac{1}{2}\sigma \tag{53}$$

where σ is the vector matrix whose components are the familiar Pauli matrices. Simple algebra then yields

$$\mathbf{B}_+ = -\mathbf{B}_- = -\frac{\mathbf{R}}{R^3} \tag{54}$$

The preceding Berry curvature $\mathbf{B}_\pm$ is the magnetic field in parameter space generated by a Dirac magnetic monopole (Dirac, 1931) of strength $\mp 1/2$. Thus, the Berry phase $\gamma_\pm(C)$ of a circuit C is given by the flux of the monopole through the surface S subtended by the circuit C, which, by Gauss' theorem, is nothing but $\mp\Omega(C)$, where $\Omega(C)$ is the solid angle described by $\mathbf{R}$ along the circuit C.

The corresponding vector potential (or Berry connection) $\mathbf{A}_\pm$ (not calculated here) has an essential singularity along a line (Dirac string) ending at the origin and carrying a 'flux' of magnitude $\pm 2\pi$. The position of the Dirac string can be moved (but not removed!) by a gauge transformation, as sketched in Figure 3. If the Dirac string happens to cross the surface S, the Berry phase remains unchanged (modulo 2π), so that the result is indeed gauge invariant.

5 EXAMPLES OF BERRY PHASE

5.1 Spin in a magnetic field

As the first example, we consider the case of a single spin (of magnitude S) in a magnetic field, which is both the most immediate application of the formal theory presented in the preceding text and one of the most frequent cases encountered in experimentally relevant situations. The Hamiltonian considered is

$$H(\mathbf{b}) \equiv -\mathbf{b}\cdot\mathbf{S} \tag{55}$$

with the magnetic field $\mathbf{b}$ being the external parameter. The eigenvalues are

$$E_n(\mathbf{b}) = -nb \tag{56}$$

with $2n$ integer and $-S \le n \le S$. For $\mathbf{b} = 0$, the $2S+1$ eigenstates are degenerate, so the circuit C has to avoid the origin. The Berry connection can be calculated using equation (49) and well-known properties of the spin operators, and one gets

$$\mathbf{B}^n(\mathbf{b}) = -n\frac{\mathbf{b}}{b^3} \tag{57}$$

which is the 'magnetic field' (in parameter space) of a monopole of strength $-n$, located at the origin. The Berry phase is thus

$$\gamma_n(C) = -n\Omega(C) \tag{58}$$

where $\Omega(C)$ is the solid angle described by the field $\mathbf{b}$ along the circuit C. For $S = 1/2$, this of course reduces to the result obtained in the preceding text for the two-level problem. Note that the Berry phase $\gamma_n(C)$ depends only on the quantum number n (projection of $\mathbf{S}$ on $\mathbf{b}$) and not on the magnitude S of the spin. Note also, that while $H(\mathbf{b})$ is the most general Hamiltonian for a spin $S = 1/2$, this is not the case for a spin $S \ge 1$; in the latter case, we restrict ourselves to a subspace of the full parameter space. If a more general Hamiltonian and a wider parameter space is considered, the simple result obtained in the preceding text would not hold any more.

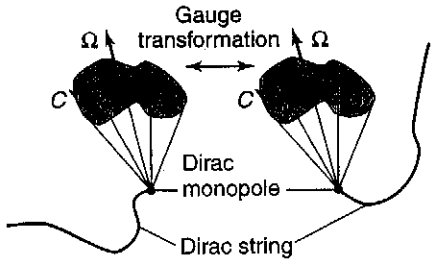

Figure 3. Sketch showing the flux of the Dirac monopole through the circuit C, and the effect of a gauge transformation.

5.2 Aharonov–Bohm effect

Another example that is of great interest, both conceptually and experimentally is the well-known Aharonov–Bohm effect (Aharonov and Bohm, 1959). We follow here the presentation of the Aharonov–Bohm effect given by Berry (1984).

Let us consider the situation depicted in Figure 4, namely, a magnetic field confined in a tube with flux Φ and a box, located at $\mathbf{R}$, in which particles of charge q are confined. The magnetic field vanishes everywhere outside the flux tube and, in particular, inside the box. Let $\mathbf{A}(\mathbf{r})$ be the corresponding vector potential. The latter generally does not vanish in the regions of vanishing field (unless the flux Φ is a multiple of the flux quantum $\Phi_0 \equiv h/e$).

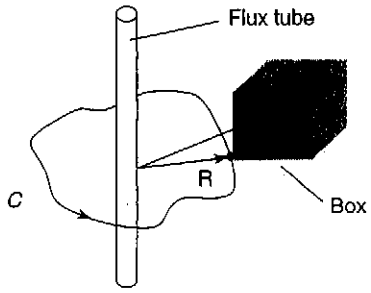

Figure 4. Sketch describing the Aharonov–Bohm effect.

Let the Hamiltonian describing the particles in the box be $H(\mathbf{p}, \mathbf{r}-\mathbf{R})$; the corresponding wave functions, for a vanishing vector potential, are of the form $\psi_n(\mathbf{r}-\mathbf{R})$, with energies E_n independent of $\mathbf{R}$. When the flux is nonzero, we can choose as basis states $|n(\mathbf{R})\rangle$, satisfying

$$H(\mathbf{p}-q\mathbf{A}(\mathbf{r}), \mathbf{r}-\mathbf{R})|n(\mathbf{R})\rangle = E_n|n(\mathbf{R})\rangle \tag{59}$$

whose solutions are given by

$$\langle \mathbf{r}|n(\mathbf{R})\rangle = \exp\left[\frac{iq}{\hbar}\int_{\mathbf{R}}^{\mathbf{r}} d\mathbf{r}'\cdot\mathbf{A}(\mathbf{r}')\right]\psi_n(\mathbf{r}-\mathbf{R}) \tag{60}$$

where the integral is performed along a path contained in the box. The energies E_n are independent of the vector potential, because it is always possible to find a gauge transformation that would make it zero in the box (but not everywhere in space!).

The Hamiltonian depends on the position $\mathbf{R}$ of the box via the vector potential. Thus, our parameter space, in this example, is nothing but the real space, with exclusion of the region of the flux tube. If we transport the box around a closed circuit C, the Berry phase will be given by

$$\gamma_n(C) \equiv \oint_C \mathbf{A}^n(\mathbf{R})\cdot d\mathbf{R} \tag{61}$$

with the Berry connection

$$\begin{aligned}\mathbf{A}^n(\mathbf{R}) &\equiv -\mathrm{Im}\left[\langle n(\mathbf{R})|\partial_{\mathbf{R}} n(\mathbf{R})\rangle\right] \\ &= -\mathrm{Im}\iiint d^3\mathbf{r}\psi_n^*(\mathbf{r}-\mathbf{R}) \\ &\quad\times\left[\frac{-iq}{\hbar}\mathbf{A}(\mathbf{R})\psi_n(\mathbf{r}-\mathbf{R}) + \partial_{\mathbf{R}}\psi_n(\mathbf{r}-\mathbf{R})\right] \\ &= \frac{q}{\hbar}\mathbf{A}(\mathbf{R})\end{aligned} \tag{62}$$

The Berry curvature $\mathbf{B}^n(\mathbf{R}) = \nabla\times\mathbf{A}^n(\mathbf{R}) = (q/\hbar)\mathbf{B}(\mathbf{R})$ is just given by the magnetic field and vanishes everywhere outside the flux tube. But because the tube region is excluded from the allowed parameter space, the latter is multiply connected, and the Berry phase is purely topological, given by the winding number $N(C)$ of the circuit C around the flux tube, and by the flux Φ

$$\gamma_n(C) = 2\pi N(C)\frac{q}{h}\Phi \tag{63}$$

The Aharonov–Bohm effect was confirmed experimentally by electron holography by Tonomura *et al.* (1986) in a configuration where the magnetic field truly vanishes, and plays an outstanding role in the physics of mesoscopic systems; here, it gives rise to conductance oscillations and to persistent currents in mesoscopic metallic rings threaded by a magnetic flux (Olariu and Popescu, 1985; Aronov and Sharvin, 1987; Washburn and Webb, 1992).

5.3 Thomas precession and spin-orbit coupling

In relativistic kinematics, space–time coordinates perceived by observers in different inertial frames are related to each other by Lorentz transformations. The latter may consist of pure Lorentz boosts, pure rotations, or combinations of a boost and a rotation. As is well known, Lorentz boosts with different velocity axes do not commute with each other, and the product of two pure Lorentz boosts with different axes is not a pure Lorentz boost but the product of a Lorentz boost and a rotation. This effect gives rise to the phenomenon of Thomas precession (Thomas, 1926, 1927), which is one of the contributions to the spin-orbit coupling (the other contribution being the result of the Lorentz transformation of the electric field).

Recently, it has been pointed out that the Thomas precession may be understood as an anholonomy associated with the parallel transport on the manifold Lorentz boosts (Jordan, 1988; Aravind, 1997; Rhodes and Semon, 2004). This important result is briefly outlined here.

For simplicity, we restrict to Lorentz boosts in the xy plane and rotations around the z axis. A Lorentz boost of velocity $\mathbf{v} \equiv (v_x, v_y)$ can be characterized by a point (ct, x, y) on the hyperboloid $(ct)^2 - (x^2+y^2) = 1$ $(t \geq 0)$, such that $(v_x, v_y) = (x/t, y/t)$. Thus a closed trajectory in the space of Lorentz boosts is characterized by a closed loop on the hyperboloid. One can show (Jordan, 1988; Aravind, 1997; Rhodes and Semon, 2004) that upon such a closed loop the system does not return to the initial inertial frame but to an inertial frame that differs from the initial one by a rotation around the z axis, of angle $\theta = -A$, where A is the area enclosed by the loop on the hyperboloid. This rotation is precisely the Thomas precession (Thomas, 1926, 1927), the geometrical nature of which appears clearly from the present formulation. For a quantum spin, a Berry phase

results from the Thomas precession. Another contribution (for charged particles) arises from the Lorentz transformation of the electric field and combines with the Thomas precession to give the familiar spin-orbit coupling of the electron.

For velocities much smaller than the velocity of light, the Berry phase corresponding to a closed loop C in the (v_x, v_y) plane due to the spin-orbit coupling (including both the Thomas precession contribution and the Lorentz transformation of the electric field) is given by the simple expression

$$\gamma_\sigma(C) = -\sigma \oint_C \frac{\mathbf{v} \times \mathrm{d}\mathbf{v}}{4c^2} = -\sigma \frac{A(C)}{4c^2} \tag{64}$$

with $\sigma = \pm 1$ for $s_z = \pm 1/2$, respectively, and where $A(C)$ is the area swept in the (v_x, v_y) plane.

The geometric character of the spin-orbit coupling appears clearly from the preceding expression. For an electron in a periodic orbit, the Berry phase accumulates linearly in time, which amounts to an additional term in the dynamical phase, that is, to the spin-orbit coupling term of the Hamiltonian, which is given by the following expression (for velocities much smaller than c):

$$H_{\mathrm{SO}} = \hbar \mathbf{s} \cdot \left(\frac{\mathbf{v} \times \mathbf{a}}{2c^2} \right) \tag{65}$$

where $\mathbf{a}$ is the acceleration.

The preceding formulation of the spin-orbit coupling allows us to understand qualitatively why electrons with group velocities much smaller than c may nevertheless have a spin-orbit splitting, several orders of magnitude larger than that of free electrons with equivalent velocity. In a quasiclassical picture, the motion of electrons in a solid may be viewed as consisting mostly of periodic orbital motion around nuclei, combined with a hopping interatomic motion. The hopping frequency from atom to atom, which determines the average electron velocity, is typically much smaller than the frequency of the intra-atomic orbital motion around the nuclei. The Berry phase accumulated between two successive hopping events, determined essentially by this intra-atomic orbital motion, is considerably larger than the one accumulated in the interatomic hopping motion, so that the effective spin-orbit coupling of Bloch electrons in a solid may be enhanced by a factor of the order of 10^4 as compared to the spin-orbit coupling of free electrons.

5.4 Experimental observations of the Berry phase for a single spin

Let us now discuss how the Berry phase could be detected experimentally. As already mentioned, this is not immediately clear since the expectation value of any observable would be independent of the phase of the system. As always, when considering phases, some kind of interference has to be observed. There are various ways in which this can be done.

- Berry's original proposal (Berry, 1984) was as follows: A monoenergetic polarized beam of particles in the spin state n along the magnetic field $\mathbf{b}$ is split into two beams. For one of the beams, the field $\mathbf{b}$ is kept constant in magnitude and direction, whereas for the second beam, the magnitude of $\mathbf{b}$ is kept constant and its direction is slowly varied along a circuit C subtending a solid angle Ω. The two beams are then recombined to interfere, and the intensity is monitored as a function of the solid angle Ω. Since the dynamical phase is the same for both beams, the phase difference between the two beams is given purely by the Berry phase (plus a propagation factor is determined by the phase shift for $\Omega = 0$). Although conceptually possible, it seems unlikely that such an experiment would be feasible in practice. In particular, it would be extremely difficult to ensure that the difference between the dynamical phases of the two beams is smaller than the Berry phase one wants to detect, unless some physical principle enforces it. This kind of experiment may be said to be of type 'one state – two Hamiltonians'. This kind of experiment, being based on interferences, is truly quantum mechanical.
- An alternative approach, more amenable to an experimental test, is to prepare the system into a superposition of two states, that is,

$$|\psi(t=0)\rangle = \alpha |n(\mathbf{R}(t=0))\rangle + \beta |m(\mathbf{R}(t=0))\rangle \tag{66}$$

with $m = n - 1$ and $|\alpha|^2 + |\beta|^2 = 1$, for example, by polarizing it along a direction perpendicular to the field $\mathbf{b}$. The orientation of the transverse component of the spin is given by the angle $\theta(t=0) \equiv \arg(\beta) - \arg(\alpha)$. The spin of course precesses at around $\mathbf{b}$ at the Larmor frequency $\omega_L = b/\hbar$. After completion of the circuit C, the system state has evolved to

$$|\psi(T)\rangle = \alpha \exp[\mathrm{i}(\delta_n + \gamma_n(C))] |n(\mathbf{R}(t=0))\rangle + \beta \exp[\mathrm{i}(\delta_m + \gamma_m(C))] |m(\mathbf{R}(t=0))\rangle \tag{67}$$

and the polarization angle has evolved to $\theta(T) = \theta(t = 0) + \Delta\theta$ with

$$\Delta\theta = \Delta\theta_{\mathrm{dyn}} + \Delta\theta_{\mathrm{B}} \tag{68}$$

$$\Delta\theta_{\mathrm{dyn}} \equiv \delta_m - \delta_n = \omega_L T \tag{69}$$

$$\Delta\theta_{\mathrm{B}} \equiv \gamma_m(C)) - \gamma_n(C)) \tag{70}$$

Here the angle $\Delta\theta_{dyn}$ gives the polarization rotation due to the Larmor precession (dynamic phase), while $\Delta\theta_B$ is the polarization rotation due to the Berry phase accumulated along the circuit C. Thus by investigating how the polarization varies as the circuit C is modified, the Berry phase can be detected. Such an experiment may be said to be of the type 'two states – one Hamiltonian'. Note that this type of experiment can be interpreted in purely classical terms (Cina, 1986) (it bears a clear analogy to the rotation of the swinging plane of the Foucault pendulum); this is related to the fact that only Berry phase differences between two states, and not the absolute Berry phase of a given state, are detected.

- A further possibility consists in repeating the circuit C in a periodic manner. Thus, the Berry phase is accumulated linearly in time, just as the dynamical phase, and leads to an apparent energy shift for the state n,

$$\Delta E_n = \frac{\hbar}{T}\gamma_n(C) \tag{71}$$

which gives rise to an observable shift of the transition between two levels n and m. Such an experiment too is of type 'two states – one Hamiltonian'. It can also be interpreted in classical terms and has close analogy to the period shift of a Foucault pendulum with circular oscillation.

The Berry phase has been observed for neutrons ($S = 1/2$) by Bitter and Dubbers (1987), who used the experiment shown in Figure 5. A slow ($v \simeq 500\,\mathrm{ms}^{-1}$), monochromatic beam of neutrons polarized ($P \simeq 0.97$) along an axis perpendicular to the beam axis z is injected in a cylinder with a helical magnetic field with longitudinal component B_z and transverse component B_1 making a right-handed turn of 2π. Depending on the values of B_z and B_1, various values of the solid angle Ω may be achieved.

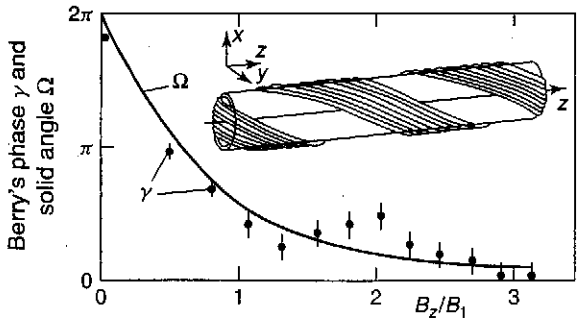

Figure 5. Measurement of Berry phase of neutrons. The inset shows the arrangement of the coil giving a helical field; the neutron beam is along z; length: 40 cm, diameter: 8 cm; an axial coil (not shown) produces a field B_z. The curve shows the Berry phase (more precisely $\gamma_{-1/2} - \gamma_{1/2}$) and solid angle Ω as a function of the ratio B_z/B_1. (Reproduced from Bitter & Dubber 1987, with permission from the American Physical Society. © 1987.)

After having traversed the cylinder, the polarization of the beam is measured, from which the Berry phase can be extracted. The comparison of the measured Berry phase (or more precisely the difference of Berry phase between states $S_z = +1/2$ and $S_z = -1/2$) and of the solid angle is shown in Figure 5. The observation is in good agreement with the theoretical prediction.

The Berry phase has also been confirmed for photons ($S = 1$) by Tomita and Chiao (1986) using an experimental procedure proposed by Chiao and Wu (1986); for protons ($S = 1/2$) by Suter, Chingas, Harris and Pines (1987) following a proposal of Moody, Shapere and Wilczek (1986); and for ^{35}Cl nuclei by Tycko (1987).

6 ANOMALOUS HALL EFFECT

The Berry phase plays an important role in the modern understanding of the anomalous Hall effect. Therefore this problem will be discussed here in a detailed manner.

6.1 Brief historical sketch and survey of the state of the art

The history of the anomalous Hall effect has been quite a turbulent one, rich in misconceptions and controversies, and the reader approaching the corresponding literature without a sufficient overview of the historical developments might easily get lost in details of controversial debates. Therefore, it appears useful to briefly sketch the main stages in the historical development of the field.

Soon after his discovery of the Hall effect of normal metals subject to an external magnetic field (Hall, 1880a), Erwin H. Hall discovered that ferromagnetic metals may exhibit a spontaneous (i.e., in the absence of an external magnetic field) Hall effect (Hall, 1880b, 1881). Toward the end of the nineteenth century and in the first half of the twentieth century, extensive experimental and phenomenological investigations of the anomalous Hall effect of ferromagnetic metals and alloys were carried out (Kundt, 1893; Smith, 1910; Perrier, 1930a,b; Pugh, Rostoker and Schindler, 1950; Smit and Volger, 1953; Pugh and Rostoker, 1953).

From these early studies, the following phenomenological description emerged. In linear response regime, the electric field $\mathbf{E}$ is linearly related to the current density $\mathbf{j}$ by

$$\mathbf{E} = \rho\mathbf{j} \tag{72}$$

with a resistivity tensor ρ (for a magnetic field and/or magnetization parallel to the z-axis) of the form

$$\rho = \begin{pmatrix} \rho_{xx} & \rho_{xy} & 0 \\ -\rho_{xy} & \rho_{xx} & 0 \\ 0 & 0 & \rho_{zz} \end{pmatrix} \tag{73}$$

The Hall effect is given by the antisymmetric part of the resistivity tensor, giving rise to a voltage that is transverse to both the current and the magnetic field (or magnetization). In a ferromagnet, the Hall resistivity $\rho_H = -\rho_{xy}$ is experimentally found to be of the form

$$\rho_H = R_0 H + R_S M \tag{74}$$

where H is the magnetic field, M, the magnetization, R_0, the normal Hall coefficient, and R_S, the anomalous Hall coefficient (the quantity of interest here). Alternatively, the Hall effect may be expressed in terms of the conductivity tensor, $\sigma \equiv \rho^{-1}$. Another important quantity measuring the Hall effect is the Hall angle θ_H (the angle between the electric field and the current) given by

$$\tan\theta_H \equiv \frac{-\sigma_{xy}}{\sigma_{xx}} = \frac{\rho_{xy}}{\rho_{xy}} \tag{75}$$

For values of the magnetic field usually available experimentally, the spontaneous contribution is usually much larger than the normal contribution in ferromagnets. In many cases, it has been found that as the temperature varies, the anomalous Hall resistivity varies as ρ_{xx}^2, which implies that the Hall conductivity σ_{xy} is essentially independent of the relaxation time.

Various mechanisms contribute to the anomalous Hall effect of homogenously magnetized systems:

- the Karplus–Luttinger mechanism (Karplus and Luttinger, 1954)
- the skew-scattering mechanism (Smit, 1955)
- the side-jump mechanism (Berger, 1970).

All three mechanisms rely on the combined effect of exchange and spin-orbit interactions. This can be easily understood from the following considerations. From the Onsager–Casimir symmetry relations (Onsager, 1931; Casimir, 1945), it follows that the antisymmetric part of the resistivity (or conductivity) tensor, that is, the Hall effect, is antisymmetric with respect to time-reversal invariance. In ferromagnets, time-reversal invariance is spontaneously broken by the appearance of the exchange splitting of the band structure. This fact, however, is not sufficient to explain the existence of the Hall effect; indeed, in the absence of spin-orbit interaction, the spin (magnetization) and orbital (electronic motion) degrees of freedom are completely independent of each other. This implies that all properties of the system (including the resistivity tensor) would be invariant under a continuous uniform rotation of the magnetization, resulting in a vanishing Hall effect. This state changes, however, when the electron motion and spin are coupled to each other via the spin-orbit coupling, so that the physical properties are no longer invariant under a global rotation of the magnetization, resulting in the possibility of a nonzero spontaneous Hall effect.

Although sharing a common microscopic origin, the three mechanisms mentioned in the preceding text are quite different in the way they depend on the electronic structure and/or on the impurities present in the ferromagnet.

The Karplus–Luttinger mechanism (Karplus and Luttinger, 1954) results from a velocity correction (the anomalous velocity) due to interband matrix elements of the velocity operator. It yields a Hall conductivity that is essentially a property of the pure Ferromagnet and (for low impurity concentration) is independent of the nature and concentration of impurities, that is, to a Hall resistivity proportional to ρ_{xx}^2, as observed in many cases. The original derivation by Karplus and Luttinger is quite involved and not really physically transparent. This, together with various other theoretical difficulties, led to misunderstanding and controversies that could be definitely lifted only quite recently, through the reinterpretation of the Karplus–Luttinger mechanism in terms of the Berry phase (Chang and Niu, 1996; Sundaram and Niu, 1999; Jungwirth, Niu and MacDonald, 2002). Interestingly, this important progress emerged from concepts developed in the context of the quantum Hall effect (Thouless, Kohmoto, Nightingale and den Nijs, 1982; Avron, Seiler and Simon, 1983; Simon, 1983; Thouless, 1984, 1994; Niu and Thouless, 1984; Niu, Thouless and Wu, 1985; Kohmoto,. 1985,1993), which allowed the interpretation of the quantized Hall conductance as a topological invariant, expressed as the integral of a Berry curvature over a closed manifold.

The skew-scattering mechanism (Smit, 1955) arises from the Mott scattering (Mott, 1929) at impurities, that is, from the fact that, owing to spin-orbit interaction, the scattering amplitude depends on the relative orientation of the spin with respect to the scattering plane. An illustrative picture of this mechanism is given in Figure 6(a) (Crépieux and Bruno, 2001). Consider an incident plane wave characterized by a wave vector $\mathbf{k}$, which is scattered by a central potential owing to, for example, impurity. In the presence of spin-orbit coupling, the amplitude of the wave packet becomes anisotropic in the sense that it depends on the relative directions of the scattered and incident waves and the spin. After a succession of scattering events, the average trajectory of the electron is deflected by a spin-dependent angle,

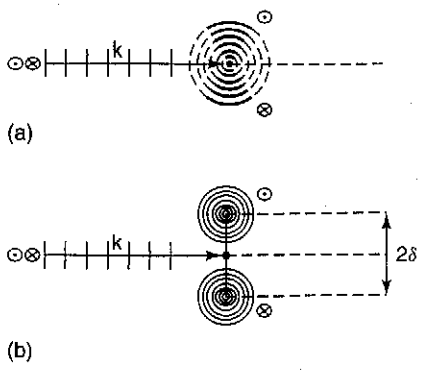

Figure 6. Sketch of the skew-scattering (a) and side-jump (b) mechanisms. (Reproduced from Crepieux & Bruno, 2001, with permission from the American Physical Society. © 2001.)

which is typically of the order of 10^{-2} rad. Because the skew scattering yields an *angular* deflection of scattered electrons, it induces a Hall angle that is *independent* of the impurity density (for sufficiently low impurity density), or in other words, a Hall resistivity that is proportional to the longitudinal resistivity.

The side-jump mechanism (Berger, 1970) arises from the fact that as a plane wave is scattered at an impurity, the outgoing scattered wave is generally not centered exactly at the impurity, but may be slightly shifted away from the impurity, as depicted in Figure 6(b) (Crépieux and Bruno, 2001). This shift can be transverse and/or longitudinal (with respect to the incident wave vector). The longitudinal shift is not directly relevant to the Hall effect and will be ignored here. The transverse shift (side jump) is due to the effect of the spin-orbit coupling and changes sign as the spin component perpendicular to the scattering plane is reversed. The existence of the side jump may be easily understood by examining the reflection of a free electron on a potential barrier under the influence of the spin-orbit coupling (Crépieux and Bruno, 2001). For free electrons, the magnitude of the side jump is of the order of $k\lambda_C{}^2/4 \simeq 10^{-15}$ m, where $\lambda_C \equiv \hbar/(mc)$ is the Compton wavelength. As pointed out by Berger (1970), and discussed in Section 5.3 in the preceding text, band-structure considerably enhance the effective spin-orbit coupling experienced by electrons in solids, and yield an enhancement factor of the order of 10^4 of the magnitude of the side jump. The side jump contributes to the Hall current in two ways: (i) the side jumps experienced at each collision add up to yield a transverse current, and (ii) in the presence of an external electric field, the side jump induces a shift of the electron distribution function away from the Dirac distribution, yielding another contribution to the transverse current (Berger, 1970). The two contributions can be shown to be identical. The most important feature of the side-jump contribution is that it yields a Hall conductivity that is independent of the impurity concentration (and, at least for s-scattering, independent of the sign and magnitude of the scattering potential). Thus, it is essentially an *intrinsic* contribution to the total Hall conductivity just like the Karplus–Luttinger term, and, therefore, yields a contribution to the Hall resistivity that is proportional to ρ_{xx}^2 (Berger, 1970).

Until recently, it was believed that spin-orbit coupling is an essential ingredient to obtain a nonvanishing anomalous Hall effect. This belief is indeed correct in uniformly magnetized ferromagnets for the reasons explained in the preceding text. However, the argument put forward to justify the necessity of the spin-orbit coupling does not hold any more for magnetic systems with noncollinear magnetization. In fact, in general, a time-reversed magnetic configuration (i.e., with all magnetic moments flipped) cannot be obtained by a global rotation of the magnetic moments, unless the magnetization is collinear or coplanar. Therefore, from symmetry considerations, a nonvanishing anomalous Hall effect may be expected, even without spin-orbit coupling, in a magnetic system with a chiral spin texture. Quite recently, it has been proposed that the chiral textured magnetic system may exhibit anomalous Hall effect not (directly) related to the spin-orbit coupling (Ye *et al.*, 1999; Ohgushi, Murakami and Nagaosa, 2000; Chun *et al.*, 2000; Taguchi and Tokura, 2001; Taguchi *et al.*, 2001, 2003, 2004; Lyanda-Geller *et al.*, 2001; Shindou and Nagaosa, 2001; Yanagihara and Salamon, 2002; Tatara and Kawamura, 2002; Onoda and Nagaosa, 2002, 2003a,b; Bruno, Dugaev and Taillefumier, 2004; Onoda, Tatara and Nagaosa, 2004; Baily and Salamon, 2005; Kézsmárki *et al.*, 2005). The mechanism responsible for the anomalous Hall effect, in this case, relies on the Berry phase accumulated as an electron moves in a textured exchange field. If the exchange splitting is large enough and the electron velocity small enough, the electron spin must adiabatically follow the direction of the local exchange field as it moves through the lattice. In the reference frame where the electron is at rest, it experiences an adiabatically moving exchange field, and the associated geometrical phase in turn generates a fictitious Aharonov–Bohm phase as the electron moves through the lattice. The electron's orbital degree of freedom is coupled to the fictitious field in exactly the same way as to a real magnetic field, and therefore also responds in the same way. In particular, it experiences a Lorentz force that can give rise to a nonvanishing anomalous Hall effect if a net chirality is present.

It is worth pointing out that the theory of the anomalous Hall effect involves the Berry phase in two distinct ways:

1. In the anomalous Hall effect of homogenous ferromagnets, the Karplus–Luttinger contribution can be interpreted as a Berry phase in momentum space.

2. In chiral textured ferromagnets, the anomalous Hall effect arises from the Berry phase due to the exchange field texture in real space.

In the following text, we shall discuss in more detail the interplay of the Berry phase and anomalous Hall effect in these two different contexts.

6.2 Berry phase and the anomalous Hall effect in homogenous ferromagnets

From Kubo's linear response theory, the conductivity tensor for independent electrons is given by Luttinger (1969)

$$\sigma_{ij} = \frac{ie^2\hbar}{\Omega}\lim_{s\to 0^+} \times \left\langle \sum_{n,m} \frac{f(\varepsilon_n) - f(\varepsilon_m)}{\varepsilon_m - \varepsilon_n} \frac{\langle n|\, v_j\, |m\rangle \langle m|\, v_i\, |n\rangle}{\varepsilon_n - \varepsilon_m + is} \right\rangle_c \quad (76)$$

In this equation, n, m label the eigenstates, the thermodynamic limit is implied (volume Ω tending to infinity), and $\langle \ldots \rangle_c$ indicates averaging over impurity configuration. For metals, particular care is needed to perform the limit $s \to 0^+$. Simply setting $s = 0$ yields the Karplus–Luttinger term. The remaining contributions arise from the vicinity of the Fermi level and yield the skew-scattering and side-jump contributions. Here, we are interested in the Karplus–Luttinger term. Disorder is usually considered to be of minor importance for the Karplus–Luttinger term and will be neglected from now on, so that the eigenstates are labeled by the band index n and the wave vector $\mathbf{k}$ in the first Brillouin zone. We thus get

$$\sigma_{ij}^{KL} = -e^2\hbar \int_{1BZ} \frac{\mathrm{d}^D\mathbf{k}}{(2\pi)^D} \sum_{n\neq m} (f(\varepsilon_n(\mathbf{k})) - f(\varepsilon_m(\mathbf{k}))) \times \frac{\mathrm{Im}\left[\langle n\mathbf{k}|\, v_j\, |m\mathbf{k}\rangle \langle m\mathbf{k}|\, v_i\, |n\mathbf{k}\rangle\right]}{(\varepsilon_n(\mathbf{k}) - \varepsilon_m(\mathbf{k}))^2} \quad (77)$$

Using the fact that, for $m \neq n$,

$$\langle n\mathbf{k}|\, H\, |m\mathbf{k}\rangle = 0 \quad (78)$$

one obtains

$$\langle \partial_{\mathbf{k}}(n\mathbf{k})|\, m\mathbf{k}\rangle\, \varepsilon_m(\mathbf{k}) + \langle n\mathbf{k}|\, \partial_{\mathbf{k}}(m\mathbf{k})\rangle\, \varepsilon_n(\mathbf{k}) + \langle m\mathbf{k}|\, \frac{\partial H(\mathbf{k})}{\partial \mathbf{k}}\, |n\mathbf{k}\rangle = 0 \quad (79)$$

Similarly, $\langle n\mathbf{k}|\ m\mathbf{k}\rangle = 0$ implies that

$$\langle \partial_{\mathbf{k}}(n\mathbf{k})|\, m\mathbf{k}\rangle + \langle n\mathbf{k}|\, \partial_{\mathbf{k}}(m\mathbf{k})\rangle = 0 \quad (80)$$

so that

$$\frac{\langle n\mathbf{k}|\, v_j\, |m\mathbf{k}\rangle}{\varepsilon_n(\mathbf{k}) - \varepsilon_m(\mathbf{k})} = \frac{1}{\hbar}\langle \partial_{k_j}(n\mathbf{k})|\ m\mathbf{k}\rangle \quad (81)$$

Finally, we get

$$\sigma_{ij}^{KL} = -\frac{2e^2}{\hbar} \int_{1BZ} \frac{\mathrm{d}^D\mathbf{k}}{(2\pi)^D} \sum_n f(\varepsilon_n(\mathbf{k}))\, \mathrm{Im} \times \left[\langle \partial_{k_j}(n\mathbf{k})|\ \partial_{k_i}(n\mathbf{k})\rangle\right] \quad (82)$$

Defining the Berry curvature in band n as

$$\boldsymbol{\Omega}^{(n)} \equiv -\mathrm{Im}\left(\langle \partial_{\mathbf{k}}(n\mathbf{k})| \times |\partial_{\mathbf{k}}(n\mathbf{k})\rangle\right) \quad (83)$$

we finally obtain

$$\sigma_{ij}^{KL} = -\frac{e^2}{\hbar} \int_{1BZ} \frac{\mathrm{d}^D\mathbf{k}}{(2\pi)^D} \sum_n f\left({}^{(n)}\varepsilon_n(\mathbf{k})\right) \varepsilon_{ijk}\Omega_k(\mathbf{k}) \quad (84)$$

where ε_{ijk} is the fully antisymmetric tensor. This result is best understood for two-dimensional systems ($D = 2$), where only σ_{xy} and $\Omega_z^{(n)}$ are of interest. There the contribution of the band of index n to the Karplus–Luttinger term is simply determined by the Berry phase associated with parallel transport (with the $\mathbf{k}$-plane playing the role of the parameter space) around the Fermi surface (which is a line in two dimensions).

The case of an insulating system is of particular interest. In this case, there are no Fermi surface contributions (skew scattering and side jump) to the Hall conductivity, and the latter thus reduces to the Karplus–Luttinger term. The contribution of the occupied bands is thus given by an integral over the whole first Brillouin zone (empty bands do not contribute). Because the first Brillouin zone may be viewed as a closed surface (torus), the conductance is topologically quantized in multiples of the quantum of conductance, e^2/h. Since the longitudinal conductance vanishes, we obtain the integer quantum Hall effect without an external magnetic field. This result is completely analogous to the quantum Hall effect obtained in the problem of the Hofstadter butterfly (Hofstadter, 1976; Thouless, Kohmoto, Nightingale and den Nijs, 1982; Avron, Seiler and Simon, 1983).

It is completely similar to the Bonnet theorem in differential geometry (Nakahara, 1990), which relates the integral of the Gaussian curvature (which is a local geometrical property) over a closed surface to its Euler index (which is a global topological invariant).

The simplest example for the Berry phase formulation of the Karplus–Luttinger term is given by the two-dimensional electron gas in the presence of Rashba spin-orbit coupling

and exchange splitting. It is described by the following Hamiltonian:

$$\mathcal{H} = \frac{\hbar^2 \mathbf{k}^2}{2m^*} + \alpha\left(\sigma_x k_y - \sigma_y k_x\right) - M\sigma_z \tag{85}$$

The eigenvalues (shown in Figure 7) are

$$E_{\mathbf{k}}^{\pm} = \frac{\hbar^2 k^2}{2m^*} \mp \lambda(k) \tag{86}$$

with

$$\lambda(k) \equiv \sqrt{M^2 + \alpha^2 k^2} \tag{87}$$

The eigenstates $|\mathbf{k}, \pm\rangle$ are polarized along (resp. against) the unit vector

$$\mathbf{n}(\mathbf{k}) \equiv \left(\frac{\alpha k_y}{\lambda(k)}, \frac{-M}{\lambda(k)}, \frac{\alpha k_y}{\lambda(k)}\right) \tag{88}$$

Thus, as one performs a closed loop around the Fermi line, the spin quantization axis describes a cone, the solid angle of which determines the Berry phase, and, hence, the Karplus–Luttinger contribution to the anomalous Hall effect. We have

$$\sigma_{xy}^{KL} = -\frac{e^2}{h}\frac{1}{4\pi}\int \mathrm{d}^2\mathbf{k}\left[f(E_{\mathbf{k}}^{+}) - f(E_{\mathbf{k}}^{-})\right]\varepsilon_{\alpha\beta\gamma} n_\alpha \frac{\partial n_\beta}{\partial k_x}\frac{\partial n_\gamma}{\partial k_y} \tag{89}$$

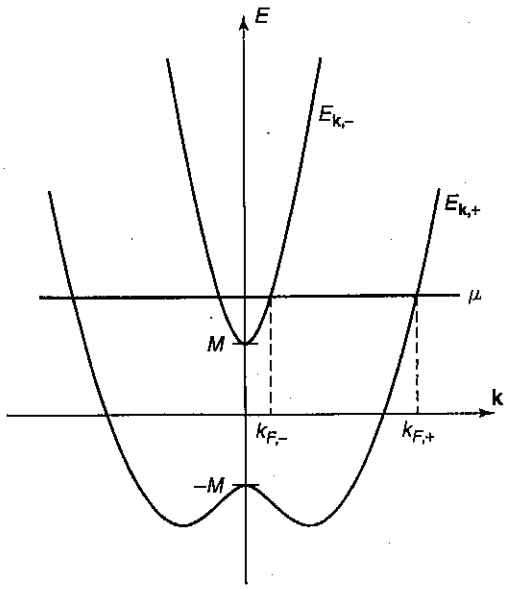

Figure 7. Energy spectrum of electrons in a two-dimensional ferromagnet with Rashba spin-orbit interaction (schematically). (Reproduced from Dugaev *et al.*, 2005, with permission from the American Physical Society. © 2005.)

which, for weak spin-orbit coupling ($\alpha k_F \ll M$), finally yields

$$\sigma_{xy}^{KL} \simeq \frac{e^2}{h}\frac{m^*\alpha^2}{M}\left[\theta(M - \varepsilon_F)\frac{\varepsilon_F + M}{2M} + \theta(\varepsilon_F - M)\right] \tag{90}$$

For more extensive discussions, the reader is referred to original publications (Jungwirth, Niu and MacDonald, 2002; Fang *et al.*, 2003; Culcer, MacDonald and Niu, 2003; Yao *et al.*, 2004; Lee *et al.*, 2004; Haldane, 2004; Sinova, Jungwirth and Černe, 2004; Dugaev *et al.*, 2005; Sinitsyn, Niu, Sinova and Nomura, 2005).

6.3 Berry phase and the anomalous Hall effect in chiral textured ferromagnets

Let us consider here a system with the Hamiltonian

$$\mathcal{H} \equiv \frac{\mathbf{p}^2}{2m^*} - \mathbf{\Delta}(\mathbf{r})\cdot\sigma \tag{91}$$

where $\mathbf{\Delta}(\mathbf{r}) \equiv \Delta(\mathbf{r})\mathbf{n}(\mathbf{r})$ is a spatially varying exchange potential. Here the quantization axis is chosen to be along z everywhere. This choice is arbitrary, however (it is in fact a gauge choice), and any other choice could be made. In particular, the exchange term becomes simpler if we choose a gauge such that the quantization axis is everywhere along $\mathbf{n}(\mathbf{r})$, that is, if we perform the unitary transformation

$$\mathcal{H} \to \tilde{\mathcal{H}} \equiv \mathcal{T}^\dagger \mathcal{H} \mathcal{T} \tag{92}$$

with

$$\mathcal{T}^\dagger(\mathbf{r})\left[\mathbf{n}(\mathbf{r})\cdot\sigma\right]\mathcal{T}(\mathbf{r}) = \sigma_z \tag{93}$$

However, we should pay attention to the fact that the unitary operator $\mathcal{T}(\mathbf{r})$ does not commute with the momentum operator $\mathbf{p} \equiv -\mathrm{i}\hbar\partial/\partial\mathbf{r}$. Thus, the price to pay for the simplification of the exchange term is a more complicated expression of the kinetic energy term, and the transformed Hamiltonian reads

$$\tilde{\mathcal{H}} = \frac{1}{2m^*}\left(\mathbf{p} + e\mathbf{A}(\mathbf{r})\right)^2 - \Delta(\mathbf{r})\sigma_z \tag{94}$$

where $\mathbf{A}(\mathbf{r})$ is a nonabelian (2×2-spinor) gauge potential given by

$$A_i(\mathbf{r}) \equiv 2\mathrm{i}\pi\phi_0 \mathcal{T}^\dagger(\mathbf{r})\partial_i \mathcal{T}(\mathbf{r}) \tag{95}$$

Note that in the definition of the gauge potential $\mathbf{A}(\mathbf{r})$, we have introduced the flux quantum $\phi_0 \equiv h/e$ for convenience, in order to be able to express the gauge potential in the same

units as a usual vector potential. It is important to realize, however, that this is merely a convention – the electron charge (being absent from the original Hamiltonian) plays no role here, and we would have obtained the same result for a neutral particle, such as the neutron.

It may seem at first sight that we have made no real progress by changing to a new gauge – the exchange has been simplified, but the kinetic energy has taken a more complicated form. However, if the exchange splitting is large enough compared to the rate of variation of $\mathbf{n}(\mathbf{r})$ (as seen in the reference frame in which the electron is at rest), spin flip terms due to the kinetic energy term become negligible, and the spin has to adiabatically follow the local direction of $\mathbf{n}(\mathbf{r})$. More precisely, the condition of adiabaticity (for an electron at the Fermi level) reads:

$$\alpha \equiv \frac{\hbar^2 k_F}{m^* \xi \Delta} \ll 1 \tag{96}$$

where ξ is the typical length on which the direction of $\mathbf{n}(\mathbf{r})$ makes a change of the order of π. If the adiabaticity condition is satisfied, the two-spin channels decouple and one gets:

$$\tilde{\mathcal{H}} = \begin{pmatrix} \tilde{\mathcal{H}}_\uparrow & 0 \\ 0 & \tilde{\mathcal{H}}_\downarrow \end{pmatrix} \tag{97}$$

with

$$\tilde{\mathcal{H}}_\sigma \equiv \frac{1}{2m^*} (\mathbf{p} + \sigma e \mathbf{a}(\mathbf{r}))^2 - \sigma \Delta(\mathbf{r}) + V(\mathbf{r}) \tag{98}$$

with $\sigma = +1$ (-1) for $\uparrow$ $(\downarrow)$, respectively, and where the effective vector and scalar potentials are respectively given by

$$a_i(\mathbf{r}) = \pi \phi_0 \frac{n_x \partial_i n_y - n_y \partial_i n_x}{1 + n_z} \tag{99}$$

and

$$V(\mathbf{r}) \equiv \frac{\hbar^2}{8m^*} \sum_{i,\mu} (\partial_i n_\mu)^2 \tag{100}$$

Thus, we have mapped the original problem onto that of spinless particles subject to spin-dependent vector and scalar potentials. The effective magnetic field associated with the effective vector potential is defined as usual by

$$\mathbf{b} = \nabla \times \mathbf{a} \tag{101}$$

and is given in terms of $n(\mathbf{r})$ by

$$b_i = \frac{\phi_0}{8\pi} \varepsilon_{ijk} \varepsilon_{\mu\nu\lambda} n_\mu (\partial_j n_\nu)(\partial_k n_\lambda) \tag{102}$$

where Einstein's convention of summation over repeated dummy indices is implied. One can check that the effective Aharonov–Bohm phase associated with a closed path in space corresponds exactly with the Berry phase for a spin 1/2 for the corresponding path in $\mathbf{n}$ space, that is, $\pm\Omega/2$, where Ω is the solid angle described by $\mathbf{n}$. This observation establishes the link between the effective magnetic field experienced by the electron because of the exchange field texture and the concept of the Berry phase.

The electron couples to the effective vector potential in exactly the same way as it would couple to a real vector potential, and therefore the same physical consequences are expected, and obtained. These effects can be classified into two categories:

- nonlocal effects due to quantum interferences, such as the Aharonov–Bohm effect and associated persistent currents; intrinsically, these effects are of quantum mechanical nature and require phase coherence.
- local effects such as the Lorentz force and it consequences like the Hall effect; these effects are *not* quantum mechanical in essence, but classical, and do not rely on phase coherence. An insightful paper by Aharonov and Stern (1992) beautifully explains how the effective Lorentz force arises in a classical description.

A good example of the anomalous Hall effect due to a chiral texture is provided by the pyrochlore compound $Nd_2Mo_2O_7$ (Taguchi *et al.*, 2001). The structure and magnetic ordering are displayed in Figure 8. The electronic transport takes place on Mo sites, which adopt a chiral 'umbrella' spin texture owing to the exchange coupling to the Nd moments. The hopping of an electron around any Mo triangle gives rise to a Berry phase related to the solid angle described by the magnetic moments, and hence to a chirality-induced anomalous Hall effect. This is corroborated by the fact that the application of a large magnetic field closes the 'umbrella' texture, thereby suppressing the solid angle and the anomalous Hall effect.

7 OUTLOOK AND CONCLUSIONS

Besides the applications that have been discussed in the preceding text, the concept of Berry phase has been of great importance to a number of topics in solid-state physics. In the theory of the fractional quantum Hall effect, the occurrence of excitations with fractional charges comes naturally out of a Berry phase argument and gives rise to the concept of *anyon* (Wilczek, 1990). In quantum Hall ferromagnets, the Berry phase gives rise to topological excitations, called *skyrmions*

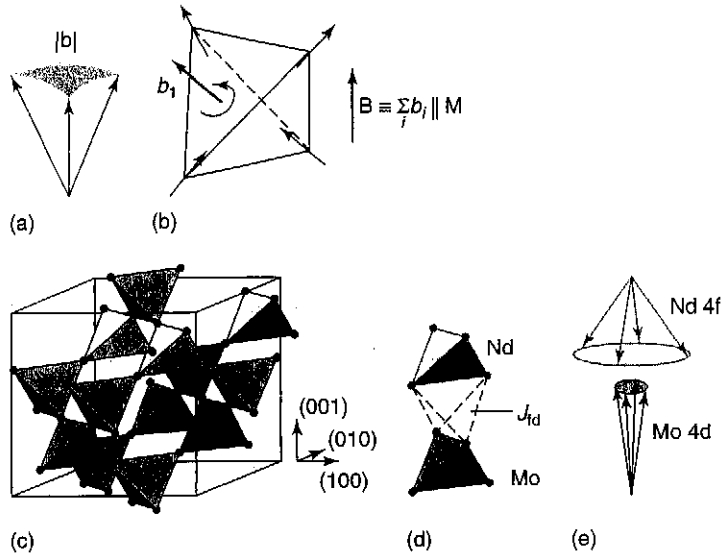

Figure 8. Schematic magnetic and crystal structures of pyrochlore. (a) Spin chirality, that is, the solid angle subtended by the three spins. (b) 'Two-in, two-out' spin structure, in which each spin points along the line that connects the center of the tetrahedron and the vertex. The total fictitious magnetic field is the vector sum of each fictitious magnetic flux that penetrates each plaquette. (c) The B sublattice of pyrochlore structure $A_2B_2O_7$. The A sublattice is structurally identical with this one, but is displaced by half a lattice constant. (d) Relative position of Nd tetrahedron (gray circles) and Mo tetrahedron (black circles) in $Nd_2Mo_2O_7$ pyrochlore. (e) The 'umbrella' structure observed for $Nd_2Mo_2O_7$ (A = Nd, B = Mo) by a neutron diffraction study. A magnetic unit cell contains four inequivalent Nd 4f moments $\mathbf{n}_i$ and four Mo 4d moments $\mathbf{m}_i$. In the umbrella structure, $(\mathbf{m}_i - \mathbf{m}) \perp \mathbf{m}$ and $(\mathbf{n}_i - \mathbf{n}) \perp \mathbf{n}$ for each $\mathbf{m}_i$ and $\mathbf{n}_i$, where $\mathbf{m}$ and $\mathbf{n}$ are the average moments of four $\mathbf{m}_i$ and four $\mathbf{n}_i$, respectively. (Reproduced from Y. Taguchi *et al*: Spin chirality, Berry phase, and anomalous Hall effect in a Frustrated Ferromagnet. *Science* **29**, (2001) 2573–76, with permission from AAAS.)

(Girvin, 1999) with novel properties. In one- and two-dimensional quantum spin systems, the physical properties depend, in a crucial manner, on whether the spin is integer or half-integer (Haldane, 1983, 1988), a phenomenon that is best understood in terms of Berry phase considerations (Loss, 1998). In molecular magnets, the Berry phase can induce destructive interferences of macroscopic tunneling between classically degenerate states, giving rise to the occurrence of *diabolical points* (Loss, DiVincenzo and Grinstein, 1992; von Delft and Henley, 1992; Garg, 1993; Wernsdorfer and Sessoli, 1999; Villain, 2003; Bruno, 2006).

The concept of the Berry phase appears as one of the most profound and insightful concepts in quantum mechanics. This article aimed at giving an introduction to this topic and illustrating its importance and versatility by means of a number of examples in the field of magnetism.

REFERENCES

Aharonov, Y. and Bohm, D. (1959). Significance of electromagnetic potentials in the quantum theory. *Physical Review*, **115**, 485–491.

Aharonov, Y. and Stern, A. (1992). Origin of the geometric forces accompanying Berry's geometric potentials. *Physical Review Letters*, **69**, 3593–3596.

Aravind, P.K. (1997). The Wigner angle as an anholonomy in rapidity space. *American Journal of Physics*, **65**, 634–636.

Aronov, A.G. and Sharvin, Y.V. (1987). Magnetic flux effects in disordered conductors. *Reviews of Modern Physics*, **59**, 755–779.

Avron, J.E., Seiler, R. and Simon, B. (1983). Homotopy and quantization in condensed matter physics. *Physical Review Letters*, **51**, 51–53.

Baily, S.A. and Salamon, M.B. (2005). Berry-phase contribution to the anomalous Hall effect in gadolinium. *Physical Review B*, **71**, 104407-1–104407-6.

Berger, L. (1970). Side-jump mechanism for the Hall effect of ferromagnets. *Physical Review B*, **2**, 4559–4566.

Berry, M.V. (1984). Quantal phases accompanying adiabatic changes. *Proceedings of the Royal Society of London Series A*, **392**, 45–57.

Berry, M.V. (1985). Classical adiabatic angles and quantal adiabatic phase. *Journal of Physics A: Mathematical and General*, **18**, 15–27.

Berry, M.V. (1990). Quantum adiabatic anholonomy. In *Anomalies, Phase, Defects*, Bregola, U.M., Marmo, G. and Morandi, G. (Eds.), Bibliopolis: Naples, pp. 125–181; also available at http://www.phy.bris.ac.uk/research/theory/Berry.

Bitter, T. and Dubbers, D. (1987). Manifestation of Berry's topological phase in neutron spin rotation. *Physical Review Letters*, **59**, 251–254.

Bohm, A., Mostafazadeh, A., Koizumi, H., *et al.* (2003). *The Geometric Phase in Quantum Systems*, Springer-Verlag: Berlin.

Bruno, P. (2006). Berry phase, topology, and degeneracies in quantum nanomagnets. *Physical Review Letters*, **96**, 117208-1–117208-4.

Bruno, P., Dugaev, V.K. and Taillefumier, M. (2004). Topological Hall effect and Berry phase in magnetic nanostructures. *Physical Review Letters*, **93**, 096806-1–096806-4.

Casimir, H.B.G. (1945). On Onsager's principle of microscopic reversibility. *Reviews of Modern Physics*, **17**, 343–350.

Chang, M.C. and Niu, Q. (1996). Berry phase, hyperorbits, and the Hofstadter spectrum: semiclassical dynamics in magnetic Bloch bands. *Physical Review B*, **53**, 7010–7023.

Chiao, R.Y. and Wu, Y.S. (1986). Manifestations of Berry's topological phase for the photon. *Physical Review Letters*, **57**, 933–936.

Chun, S.H., Salamon, M.B., Lyanda-Geller, Y., *et al.* (2000). Magnetotransport in manganites and the role of quantal phases: theory and experiment. *Physical Review Letters*, **84**, 757–760.

Cina, J.A. (1986). Classical adiabatic angle and geometric phase in spin precession. *Chemical Physics Letters*, **132**, 393–395.

Crépieux, A. and Bruno, P. (2001). Theory of the anomalous Hall effect from the Kubo formula and the Dirac equation. *Physical Review B*, **64**, 014416-1–014416-16.

Culcer, D., MacDonald, A.H. and Niu, Q. (2003). Anomalous Hall effect in paramagnetic two-dimensional systems. *Physical Review B*, **68**, 045327-1–045327-9.

von Delft, J. and Henley, C.H. (1992). Destructive quantum interference in spin tunnelling problems. *Physical Review Letters*, **69**, 3236–3239.

Dirac, P.A.M. (1931). Quantised singularities in the electromagnetic field. *Proceedings of the Royal Society of London Series A*, **133**, 60–72.

Dugaev, V.K., Bruno, P., Taillefumier, M., *et al.* (2005). Anomalous Hall effect in a two-dimensional electron gas with spin-orbit interaction. *Physical Review B*, **71**, 224423-1–224423-8.

Fang, Z., Nagaosa, N., Takahashi, K.S., *et al.* (2003). The anomalous Hall effect and magnetic monopoles in momentum space. *Science*, **302**, 92–95.

Garg, A. (1993). Topologically quenched tunnel splitting in spin systems without Kramers' degeneracy. *Europhysics Letters*, **22**, 205–210.

Girvin, S.M. (1999). Quantum Hall effect: novel excitations and broken symmetries. In *Topological Aspects of Low Dimensional Systems*, Comtet, A., Jolicoeur, T., Ouvry, S. and David, F. (Eds.), Springer-Verlag: Berlin.

Haldane, F.M.D. (1983). Nonlinear field theory of large-spin Heisenberg Antiferromagnets: semiclassically quantized solitons of the one-dimensional easy-axis Néel state. *Physical Review Letters*, **50**, 1053–1056.

Haldane, F.M.D. (1988). O(3) nonlinear σ model and the topological distinction between integer-and-half-integer-spin antiferromagnets in two dimensions. *Physical Review Letters*, **61**, 1029–1032.

Haldane, F.M.D. (2004). Berry curvature on the fermi surface: anomalous Hall effect as a topological fermi-liquid property. *Physical Review Letters*, **93**, 206602-1–206602-4.

Hall, E.H. (1880a). On a new action of the magnet on electric currents. *Philosophical Magazine*, **9**, 225–230.

Hall, E.H. (1880b). On the new action of magnetism on a permanent electric current. *Philosophical Magazine*, **10**, 301–328.

Hall, E.H. (1881). On the "rotational coefficient" in nickel and cobalt. *Philosophical Magazine*, **12**, 157–172.

Hannay, J.H. (1985). Angle variable holonomy in adiabatic excursion of an integrable Hamiltonian. *Journal of Physics A: Mathematical and General*, **18**, 221–230.

Hofstadter, D.R. (1976). Energy levels and wave functions of Bloch electrons in rational and irrational magnetic fields. *Physics Review B*, **14**, 2239–2249.

Jordan, T.F. (1988). Berry phases and unitary transformations. *Journal of Mathematical Physics*, **29**, 2042–2052.

Jungwirth, T., Niu, Q. and MacDonald, A.H. (2002). Anomalous Hall effect in ferromagnetic semiconductors. *Physical Review Letters*, **88**, 227208-1–227208-4.

Karplus, R. and Luttinger, J.M. (1954). Theory of the Hall effect in ferromagnetic substances. *Physical Review*, **95**, 1154–1160.

Kézsmárki, I., Onoda, S., Taguchi, Y., *et al.* (2005). Magneto-optical effect induced by spin chirality of the itinerant ferromagnet $Nd_2Mo_2O_7$. *Physical Review B*, **72**, 094427-1–094427-6.

Kohmoto, M. (1985). Topological invariant and the quantization of the hall conductance. *Annals of Physics*, **160**, 343–354.

Kohmoto, M. (1993). Berry's phase of Bloch electrons in electromagnetic fields. *Journal of the Physical Society of Japan*, **62**, 659–663.

Kundt, A. (1893). Das Hall'sche Phänomen in Eisen, Kobalt, und Nickel. *Annalen der Physik (Leipzig)*, **49**, 257–271.

Lee, W.L., Watauchi, S., Miller, V.L., *et al.* (2004). Dissipationless anomalous Hall current in the ferromagnetic spinel $CuCr_2Se_{4?x}Br_x$. *Science*, **303**, 1647–1649.

Loss, D. (1998). Quantum dynamics in mesoscopic magnetism. In *Dynamical Properties of Unconventional Magnetic Systems*, Skjeltorp, A.P. and Sherrington, D. (Eds.), Kluwer Academic Publishers: The Netherlands, pp. 29–75.

Loss, D., DiVincenzo, D.P. and Grinstein, G. (1992). Suppression of tunnelling by interference in half-integer-spin particles. *Physical Review Letters*, **69**, 3232–3236.

Luttinger, J.M. (1969). Transport theory. In *Mathematical Methods in Solid State and Superfluid Theory*, Clark, R.C. and Derrick, G.H. (Eds.), Oliver and Boyd: Edinburgh, pp. 157–193.

Lyanda-Geller, Y., Chun, Y., Salamon, M.B., *et al.* (2001). Charge transport in manganites: hopping conduction, the anomalous Hall effect, and universal scaling. *Physical Review B*, **63**, 184426-1–184426-27.

Mead, C.A. and Truhlar, D.G. (1979). On the determination of the Born-Oppenheimer nuclear motion wave functions including complications due to conical intersections and identical nuclei. *Journal of Chemical Physics*, **70**, 2284–2296.

Messiah, A. (1991). *Quantum Mechanics*, North Holland: Amsterdam, Vol. 2.

Moody, J., Shapere, A. and Wilczek, F. (1986). Realizations of magnetic-monopole gauge fields: diatoms and spin precession. *Physical Review Letters*, **56**, 893–896.

Mott, N.F. (1929). The scattering of fast electrons by atomic nuclei. *Proceedings of the Royal Society of London Series A*, **124**, 425–441.

Nakahara, M. (1990). *Geometry, Topology, and Physics*, Institute of Physics Publishing: Bristol.

von Neumann, J. and Wigner, E.P. (1929). Über das Verhalten von Eigenwerten bei adiabatischen Prozessen. *Physikalische Zeitschrift*, **30**, 467–470.

Niu, Q. and Thouless, D.J. (1984). Quantised adiabatic charge transport in the presence of substrate disorder and many-body interaction. *Journal of Physics A: Mathematical and General*, **17**, 2453–2462.

Niu, Q., Thouless, D.J. and Wu, Y.S. (1985). Quantized Hall conductance as a topological invariant. *Physical Review B*, **31**, 3372–3377.

Ohgushi, K., Murakami, S. and Nagaosa, N. (2000). Spin anisotropy and quantum Hall effect in the kagomé lattice: chiral spin state based on a ferromagnet. *Physical Review B*, **62**, R6065–R6068.

Olariu, S. and Popescu, I.I. (1985). The quantum effects of electromagnetic fluxes. *Reviews of Modern Physics*, **57**, 339–436.

Onoda, M. and Nagaosa, N. (2002). Topological nature of anomalous Hall effect in ferromagnets. *Journal of the Physical Society of Japan*, **71**, 19–22.

Onoda, M. and Nagaosa, N. (2003a). Spin chirality fluctuations and anomalous Hall effect in itinerant ferromagnets. *Physical Review Letters*, **90**, 196602-1–196602-4.

Onoda, M. and Nagaosa, N. (2003b). Quantized anomalous Hall effect in two-dimensional ferromagnets: quantum Hall effect in metals. *Physical Review Letters*, **90**, 206601-1–206601-4.

Onoda, M., Tatara, G. and Nagaosa, N. (2004). Anomalous Hall effect and skyrmion number in real and momentum spaces. *Journal of the Physical Society of Japan*, **73**, 2624–2627.

Onsager, L. (1931). Reciprocal relations in irreversible processes. II. *Physical Review*, **38**, 2265–2279.

Pancharatnam, S. (1956). Generalized theory of interference, and its application. *Proceedings of the Indian Academy of Sciences*, **44**, 247–262. (Also reprinted in Shapere and Wilczek, 1989.)

Perrier, A. (1930a). Grandeurs et formules théoriques nouvelles pour les phénomènes galvanomagnétiques et thermomagnétiques. *Helvetica Physica Acta*, **3**, 317–328.

Perrier, A. (1930b). Interprétation unitaire des particularités de la conduction des milieux ferromagnétiques. *Helvetica Physica Acta*, **3**, 400–427.

Pugh, E.M. and Rostoker, N. (1953). Hall effect in ferromagnetic materials. *Reviews of Modern Physics*, **25**, 151–157.

Pugh, E.M., Rostoker, N. and Schindler, A. (1950). On the Hall effect in ferromagnetics. *Physical Review*, **80**, 688–692.

Rhodes, J.A. and Semon, M.D. (2004). Relativistic velocity space, Wigner rotation and Thomas precession. *American Journal of Physics*, **72**, 943–960.

Shapere, A. and Wilczek, F. (Eds.) (1989). *Geometric Phases in Physics*, World Scientific: Singapore.

Shindou, R. and Nagaosa, N. (2001). Orbital ferromagnetism and anomalous Hall effect in antiferromagnets on the distorted fcc lattice. *Physical Review Letters*, **87**, 116801-1–116801-4.

Simon, B. (1983). Holonomy, the quantum adiabatic theorem and Berry's phase. *Physical Review Letters*, **51**, 2167–2170.

Sinova, J., Jungwirth, T. and Černe, J. (2004). Magneto-transport and magneto-optical properties of ferromagnetic (III,Mn)V semiconductors: a review. *International Journal of Modern Physics. B*, **18**, 1083–1118.

Sinitsyn, N.A., Niu, Q., Sinova, J. and Nomura, K. (2005). Disorder effects in the anomalous Hall effect induced by Berry curvature. *Physical Review B*, **72**, 045346-1–045346-11.

Smit, J. and Volger, J. (1953). Spontaneous Hall effect in ferromagnetics. *Physical Review*, **92**, 1576–1577.

Smit, J. (1955). The spontaneous Hall effect in ferromagnetics I. *Physica*, **21**, 877–887.

Smith, A.W. (1910). The variation of the Hall effect in metals with change of temperature. *Physical Review*, **30**, 1–34.

Sundaram, G. and Niu, Q. (1999). Wave-packet dynamics in slowly perturbed crystals: gradient corrections and Berry-phase effects. *Physical Review B*, **59**, 14915–14925.

Suter, D., Chingas, G.C., Harris, R.A. and Pines, A. (1987). Berry's phase in magnetic resonance. *Molecular Physics*, **61**, 1327–1340.

Taguchi, Y., Oohara, Y., Yoshizawa, H., *et al.* (2001). Spin chirality, Berry phase, and anomalous Hall effect in a frustrated ferromagnet. *Science*, **291**, 2573–2576.

Taguchi, Y., Oohara, Y., Yoshizawa, H., *et al.* (2004). The spin chirality induced anomalous Hall effect in pyrochlore ferromagnets. *Journal of Physics. Condensed Matter*, **16**, S599–S606.

Taguchi, Y., Sasaki, T., Awaji, S., *et al.* (2003). Magnetic field induced sign reversal of the anomalous Hall effect in a pyrochlore ferromagnet $Nd_2Mo_2O_7$: evidence for a spin chirality mechanism. *Physical Review Letters*, **90**, 257202-1–257202-4.

Taguchi, Y. and Tokura, Y. (2001). Enhancement of anomalous Hall effect in a filling-changed pyrochlore-type molybdate. *Europhysics Letters*, **54**, 401–406.

Tatara, G. and Kawamura, H. (2002). Chirality-driven anomalous Hall effect in weak coupling regime. *Journal of the Physical Society of Japan*, **71**, 2613–2616.

Thomas, L.H. (1926). The motion of the spinning electron. *Nature*, **117**, 514.

Thomas, L.H. (1927). The kinematics of an electron with an axis. *Philosophical Magazine*, **3**, 1–22.

Thouless, D.J. (1984). Quantized Hall effect in two-dimensional periodic potentials. *Physics Reports*, **110**, 279–291.

Thouless, D.J. (1994). Topological interpretations of quantum Hall conductance. *Journal of Mathematical Physics*, **35**, 5362–5372.

Thouless, D.J., Kohmoto, M., Nightingale, M.P. and den Nijs, M. (1982). Quantized Hall conductance in a two-dimensional periodic potential. *Physical Review Letters*, **49**, 405–408.

Tomita, A. and Chiao, R.Y. (1986). Observation of Berry's topological phase by using an optical fiber. *Physical Review Letters*, **57**, 937–940.

Tonomura, A., Osakabe, N., Matsuda, T., *et al.* (1986). Evidence for Aharonov-Bohm effect with magnetic field completely shielded from electron wave. *Physical Review Letters*, **56**, 792–795.

Tycko, R. (1987). Adiabatic rotational splittings Berry's phase in nuclear quadrupole resonance. *Physical Review Letters*, **58**, 2281–2284.

Villain, J. (2003). Magnétisme des cristaux de molécules à grand spin. *Annales de Physique*, **28**, 1–96.

Washburn, S. and Webb, R.A. (1992). Quantum transport in small disordered from the diffusive to the ballistic regime. *Reports on Progress in Physics*, **55**, 1311–1383.

Wernsdorfer, W. and Sessoli, R. (1999). Quantum phase interference and parity effects in magnetic molecular clusters. *Science*, **284**, 133–135.

Wilczek, F. (1990). *Fractional Statistics and Anyon Superconductivity*, World Scientific: Singapore.

Yanagihara, H. and Salamon, M.B. (2002). Skyrmion strings and the anomalous Hall effect in CrO_2. *Physical Review Letters*, **89**, 187201-1–187201-4.

Yao, Y., Kleinman, L., MacDonald, A.H., *et al.* (2004). First principles calculation of anomalous Hall conductivity in ferromagnetic bcc Fe. *Physical Review Letters*, **92**, 037204-1–037204-4.

Ye, J., Kim, Y.B., Millis, A.J., *et al.* (1999). Berry phase theory of the anomalous Hall effect: application to colossal magnetoresistance manganites. *Physical Review Letters*, **83**, 3737–3740.

FURTHER READING

Dirac, P.A.M. (1948). The theory of magnetic poles. *Physical Review*, **74**, 817–830.

Hofstadter, D.R. (1983). Energy levels and wave functions of Bloch electrons in rational and irrational magnetic fields. *Physical Review B*, **14**, 2239–2249.